



# Fabrication of thermo-responsive Janus silica nanoparticles and the structure–performance relationship in Pickering emulsions

Xiaoxuan Li<sup>1</sup> · Yuanyuan Wang<sup>2</sup> · Qingfeng Hou<sup>2</sup> · Wangfeng Cai<sup>1</sup> · Yan Xu<sup>1</sup> · Yujun Zhao<sup>1</sup> 

Received: 6 March 2021 / Accepted: 8 May 2021 / Published online: 27 May 2021  
© The Author(s), under exclusive licence to Springer Nature B.V. 2021

## Abstract

The application of thermal-responsive Janus particles as emulsion stabilizers in oil–water systems has attracted increasing attention in recent years. This work reported a novel Janus silica nanoparticle with one silanol side and one poly(N-isopropylacrylamide) (PNIPAM) side, which was fabricated via combining interfacial synthesis method and single-electron transfer living radical polymerization (SET-LRP) process. Their structure and surface properties were identified by SEM, TEM, <sup>1</sup>H NMR, FTIR, and TGA. The thermo-responsive performance of Janus nanoparticles in oil–water Pickering emulsion systems was also investigated as well as their emulsification properties in both the tetradecane–water and crude oil–water systems. The solubility of both Janus and symmetric PNIPAM-modified silica nanoparticles in water presents reversible thermal-responsive properties. Notably, the Janus nanoparticles show a higher phase transition temperature than the symmetric nanoparticles because the presence of silanol on one side of the Janus nanoparticles enhances its hydrophilicity due to the stronger hydrogen bond at high temperature. In comparison with symmetric nanoparticles, Janus nanoparticles exhibit superior emulsification performance in the tetradecane–water system as a result of their lower surface

---

Xiaoxuan Li and Yuanyuan Wang are co-first authors of this article.

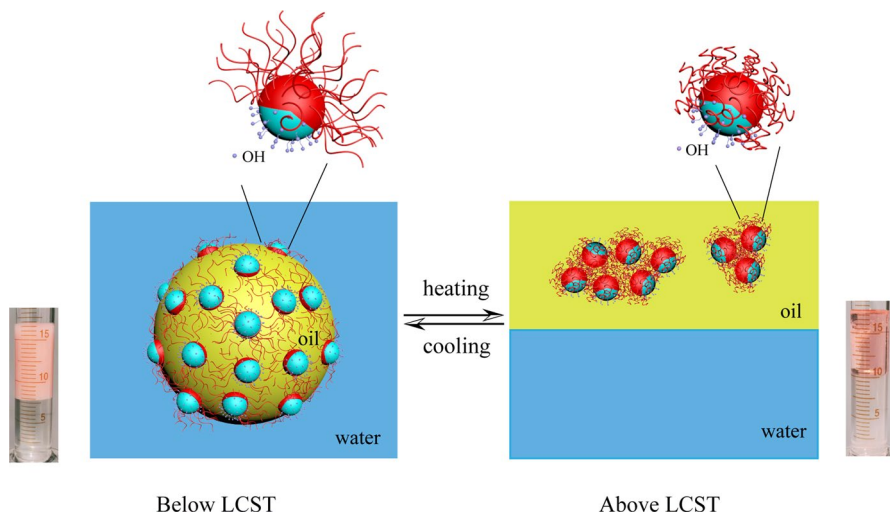
- 
- ✉ Qingfeng Hou  
houqingfeng@petrochina.com.cn
  - ✉ Yan Xu  
xuyan040506@tju.edu.cn
  - ✉ Yujun Zhao  
yujunzhao@tju.edu.cn

<sup>1</sup> Key Laboratory for Green Chemical Technology of Ministry of Education, Collaborative Innovation Center of Chemical Science and Engineering, School of Chemical Engineering and Technology, Tianjin University, Tianjin 300072, China

<sup>2</sup> Research Institute of Petroleum Exploration and Development (RIPED), CNPC, Beijing 100083, China

tension. Janus nanoparticles also present excellent thermal-responsive emulsification performance in the crude oil–water system, showing a prospective future in industrial application as a surfactant.

### Graphical abstract



**Keywords** Thermo-responsive · Janus particles · Surfactant · Silica nanoparticles · N-isopropylacrylamide

### Introduction

Janus particles, proposed after the double-faced Roman god Janus by de Gennes as early as the 1990s [1], have been more and more attractive in recent years. Janus particles not only have asymmetric structures but possess unique physical and chemical properties due to their anisotropic structures, making it possible to realize multiple functionalities and be used as catalysts, nanomotors, emulsion stabilizers and biomedicines [2–7].

Among a large number of examples of Janus particles reported previously, polymer/inorganic Janus particles have been widely studied. The polymer chains grafted on the surface of Janus particles mainly affect their chemical properties. Thus, when stimuli-responsive polymers are grafted, the nanoparticles can be defined as functional materials and show chemical or physical changes induced by external stimuli, such as pH [8–11], CO<sub>2</sub>/N<sub>2</sub> [12, 13], temperature [14–16] and redox reagents [17, 18]. Temperature is a kind of common external stimuli, which is easy to be controlled. PNIPAM is a kind of extensively studied thermo-sensitive polymer, which shows a lower critical solution temperature (LCST) of about 32 °C [19, 20]. Holderer et al. [14, 21] produced “raspberry” like composite

materials consisting of PNIPAM microgels and silica nanoparticles, which were observed to be a silica nanoparticle layer around the microgel core. Chen et al. [22] prepared  $\text{SiO}_2$ @PNIPAM NPs via nitrogen-aeration tuned ultrasonic, which exhibited obvious thermal responsive properties when used as stabilizers to form Pickering emulsions. Wu et al. [23] fabricated a kind of hybrid nanoparticles by grafting PNIPAM chains onto silica nanoparticles and revealed their temperature-induced phase transition behavior in water. Compared with symmetric particles, Janus particles present outstanding performance as emulsion stabilizers. Brink et al. [24] found that Janus particles remained high surface active even when the average contact angle was  $0^\circ$  or  $180^\circ$ , indicating their efficient emulsion stabilized ability.

Thermal-responsive Janus particles have been prepared by various synthesis methods such as polymer single-crystal templating (PSCryT) method [25–27], microfluidic synthesis [6, 28], self-assembly [29, 30] and phase separation method [31, 32]. Even though various techniques for the synthesis of Janus nanoparticles have been achieved, it is still important to find a simple and inexpensive method for quantitatively synthesizing Janus particles. For these purposes, the interfacial syntheses have been widely studied for preparing Janus particles in large production. Steve Granick and co-workers [33–35] developed a simple and typical method (interfacial synthesis) to prepare Janus particles based on Pickering emulsion, which is favorable for the selective modification processes. Chu et al. [36] studied the interfacial synthesis method proposed by Granick and developed an ideal experimental conditions for the synthesis of Janus particles with satisfactory quality. Using Granick's method, Berger et al. [9] prepared stimuli-responsive Janus particles grafted with two kinds of polymer brushes, which exhibited remarkable pH-responsive and thermo-responsive performance. Esmail et al. [37] improved the interfacial synthesis method by using a heat-driven buoyancy flow to force the dispersed nanoparticles to be placed at the wax-water interface, and successfully synthesized Janus silica nanoparticles with one (3-aminopropyl)triethoxysilane (APTES) side and one hexadecyltrimethoxysilane (HDTMS) side. Wu et al. [7] synthesized amphiphilic Janus silica nanoparticles using the interfacial synthesis method, which brought 15.74% increase in the oil recovery rate when these nanoparticles were employed as the flooding agent. Wang et al. [38] used layered alpha-zirconium phosphate (ZrP) disks and PNIPAM to prepare Janus and Gemini ZrP–PNIPAM nanoplates which proved to be thermo-responsive Pickering emulsifiers. However, few studies were focused on PNIPAM-modified Janus silica nanoparticles, and their thermal-responsive performance in oil/water systems is unclear yet. Diego et al. [39] produced multi-responsive Janus particles by partially functionalizing the surface of  $\text{Fe}_3\text{O}_4$ @ $\text{SiO}_2$  nanoparticles with poly(vinylimidazole) and PNIPAM. They mainly focused on the synthesis of Janus nanoparticles and revealed that the as-prepared Janus nanoparticles could respond against thermal, magnetic and pH stimuli in aqueous solutions, while the thermo-responsive emulsifying ability of the Janus particles in the oil/water system was not reported. Berger et al. [9] also fabricated a kind of silica-based PNIPAM Janus particles, but their studies did not mention the emulsification capability. Therefore, the emulsification capability of silica-based PNIPAM Janus

nanoparticles and their thermo-sensitive mechanism in Pickering emulsion is still an unknown problem.

In this work, a new kind of thermal-responsive PNIPAM-modified silica nanoparticles with asymmetric structure was prepared by combining Pickering emulsion-based interfacial protection method and SET-LRP process. In comparison with symmetrically PNIPAM-modified silica nanoparticles, the as-prepared Janus nanoparticles exhibit smart thermo-responsive properties and outstanding emulsification/demulsification performances. And the mechanism for thermo-responsive performance of Janus HO–SiNP–PNIPAM nanoparticles in oil–water system was also proposed. Moreover, temperature-responsive properties of the Janus nanoparticles in crude oil–water system were demonstrated.

## Experimental section

### Materials and methods

#### Materials

Tetraethoxysilane (TEOS), ammonia (25%) and n-hexane (97%) were provided by Kermel. 2-bromoisobutyryl bromide (BIBB, 98%), tetrahydrofuran (THF, 99%) and triethylamine (TEA, 99.5%) were purchased from Aladdin and THF was dried with zeolite before used. The paraffin wax (melting point of 52–54 °C) was the product of Tianjin Yuanli. Cupric bromide (CuBr<sub>2</sub>, 99%) was purchased from Macklin. L-ascorbic acid (AA) and chloroform (CDCl<sub>3</sub>, 99%) were provided by Tianjin Damao. 3-aminopropyltriethoxysilane (APTES, 98%), tris (2-dimethylaminoethyl) amine (Me6TREN, 99%), didodecyldimethylammonium bromide (DDAB, 98%) and Nisopropylacrylamide (NIPAM, 99%) were purchased from JK Chemical. As for the crude oil from Saudi Arabia, the viscosity is 43.64 mPa·s at 20 °C, the API is 26.6 and the acid number value is 0.227 mg KOH/g.

#### Preparation of silica nanoparticles

Silica nanoparticles (SiNPs) in this work were synthesized by the classic Stöber method [40]. Ammonia (25%, 20 mL) and ethanol (125 mL) were added into a three-necked round-bottom flask at room temperature. Tetraethoxysilane (TEOS, 8 mL) was then added into the flask with a stirring speed of 300 r/min, and the mixture solution was stirred at 700 r/min for 20 h. Then, the SiNPs were obtained by the centrifugation of the mixture at 8000 r/min and washed by ethanol and deionized water to remove ammonia and unreacted TEOS. Finally, the obtained SiNPs were dried in a vacuum oven overnight (50 °C). Before chemical modification, SiNPs were treated with piranha solution (30% hydrogen peroxide: concentrated sulfuric acid = 1:3) at 90 °C to enhance the formation of more surface hydroxyl groups [33].

## Preparation of Janus silica nanoparticles

*Preparation of BIBB-APTES.* APTES (0.2 mL, 0.85 mmol) and TEA (0.12 mL, 0.85 mmol), dried THF (10 mL) were put in a round-bottom flask, which was then placed into an ice bath. BIBB (0.11 mL, 0.85 mmol) and dried THF (5 mL) were added into the round-bottom flask dropwise through a dropping funnel. After stirring for 12 h at a rate of 300 r/min, the mixture was filtrated to obtain the residue, and then to remove the solvent THF, the residue was dried by a rotary evaporator. The obtained products (BIBB-APTES) were then dispersed in 50 mL of methanol.

*Preparation of Initiator-Modified Janus Silica Nanoparticles.* We prepared wax particles based on particle-stabilized emulsions using the interfacial synthesis method proposed by Granick and co-workers [33, 34]. In this process, the wax particle surface was covered by silica nanoparticles, allowing the partial exposure of the silica surface. Next, the obtained wax particles and 50  $\mu$ L ammonia were added to the methanol solution of BIBB-APTES mentioned above. After stirring the mixture for 12 h at 40 °C, the wax particles were filtrated and washed with deionized water to remove unattached nanoparticles. Then chloroform was used to dissolve wax at room temperature. The resulting silica nanoparticles were collected by centrifugation at 8000 r/min and washed by chloroform and deionized water three times, respectively. Finally, the initiator-modified Janus SiNPs (HO-SiNP-Br) were dried in a vacuum oven at 50 °C overnight.

*Preparation of PNIPAM-Modified Janus SiNPs via Single-Electron Transfer Living Radical Polymerization (SET-LRP).* The PNIPAM-modified Janus SiNPs (HO-SiNP-PNIPAM) were prepared by a SET-LRP process.  $\text{CuBr}_2$  (0.192 g, 0.85 mmol) and AA (0.06 g, 0.34 mmol) were added into Schlenk flask I and dissolved in water (15 mL). Then, Me6TREN (0.461 mL, 1.70 mmol) was dropped into Schlenk flask I under magnetic stirring at 400 r/min. Janus HO-SiNP-Br initiator (0.5 g) and NIPAM (4.836 g, 42 mmol) were also dissolved by ultrasonication in water (30 mL) in Schlenk flask II. Schlenk flask I and Schlenk flask II were degassed by three pump-inflate cycles. After that, the solution in Schlenk flask II was added into the Schlenk flask I under the protection of inert gas such as  $\text{N}_2$ . Then, the Schlenk flask I was sealed and stirred at room temperature for 7 h. Finally, the product was isolated via centrifugation at 8000 r/min and washed by deionized water three times to remove the unreacted materials. The PNIPAM-grafted Janus SiNPs (HO-SiNP-PNIPAM) were acquired after vacuum drying at 50 °C overnight.

## Preparation of symmetrically modified silica nanoparticles

*Preparation of BIBB-APTES.* The synthesis of BIBB-APTES was the same as the method mentioned above. The amounts of raw materials were as follows: APTES (1.03 mL, 4.4 mmol), TEA (0.61 mL, 4.4 mmol) and BIBB (0.56 mL, 4.4 mmol). The obtained products were then dispersed in 50 mL of methanol.

*Preparation of Initiator-Modified Silica Nanoparticles.* The above methanol solution was heated to 40 °C followed by adding 50  $\mu$ L ammonia. Then, 2.5 g of SiNPs was dispersed into the mixture solution. After stirring at 400 r/min for 12 h, the

product was collected by centrifugation. After vacuum drying at 50 °C, the initiator-modified SiNPs (SiNP–Br) were obtained.

*Preparation of PNIPAM-Modified Symmetric SiNPs via SET-LRP.* The grafting of PNIPAM was similar to the synthesis for Janus nanoparticles mentioned above. The amounts of raw materials were as followed: CuBr<sub>2</sub> (0.148 g, 0.66 mmol), AA (0.046 g, 0.264 mmol), Me6TREN (0.356 mL, 1.32 mmol), SiNP–Br initiator (0.5 g) and NIPAM (3.734 g, 33 mmol). The obtained PNIPAM-grafted symmetric SiNPs (SiNP–PNIPAM) were then dried in a vacuum oven at 50 °C overnight.

## Characterization

Scanning electron microscopy (SEM) experiments were conducted using a Hitachi Regulus 8100 field-emission SEM. The samples were treated by a Cressington sputter coater 108 auto to be coated with platinum in advance. Transmission electron microscope (TEM) images of the nanoparticles were obtained on a JEM2100 TEM. <sup>1</sup>H nuclear magnetic resonance (<sup>1</sup>H NMR) spectroscopy was measured on a VARIAN INOVA 500 MHz spectrometer using CDCl<sub>3</sub> as the solvent. Fourier transform infrared (FTIR) spectroscopy experiments were carried on a Nicolet 6700 spectrophotometer using potassium bromide (KBr) pellets. Thermogravimetric analysis (TGA) was carried out in an air atmosphere on a NETZSCH TGA 209 F3 in which the heating rate was 10 °C/min from 25 to 800 °C. To obtain the molecular weight and molecular weight distribution of grafted PNIPAM chains, about 0.3 g of HO–SiNP–PNIPAM or SiNP–PNIPAM was treated with hydrofluoric acid (HF) to cleave the grafted PNIPAM chains, then gel permeation chromatography (GPC) was conducted at 35 °C by a Viscotek TDA 305 (Malvern Instruments Ltd.), and THF was used as the eluent. Surface tension measurements of both Janus and symmetric nanoparticles aqueous solutions were determined by a POWEREACH JK99CN surface tensiometer using the Wilhelmy plate method at 25 °C. Optical transmittance of both Janus and symmetric nanoparticles aqueous solutions (0.01 wt%) was measured on a PGENERAL T6 UV–Vis spectrophotometer at 500 nm. The temperature at which the optical transmittance changes suddenly represented the phase transition temperature of the solutions.

## Results and discussion

### Synthesis of PNIPAM-modified Janus SiNPs and the mechanism

The preparation of Janus particles in this work is based on particle-stabilized emulsions (Pickering emulsions), and the synthesis route is demonstrated in Scheme 1. First, we prepared bare silica nanoparticles (SiNPs) using the classic Stöber method [40]. As shown in Fig. 1a, c, the original SiNPs present a spherical structure with a uniform particle size distribution (average diameter ~260 nm). Generally, the size of SiNPs will be affected by factors, e.g. the concentration of TEOS, ammonia, and reaction temperature [41]. By adjusting these parameters, spherical SiNPs with





different sizes can be obtained. In this work, the SiNPs with an average diameter of ~260 nm were successfully prepared when the volume ratio of TEOS: ammonia: ethanol was 1.6:4:25.

The SiNPs were treated with piranha solution to create more surface hydroxyl groups. Janus particles were then prepared using the interfacial synthesis method based on Pickering emulsions proposed by Granick and co-workers [33, 34]. It is well known that particles will be adsorbed at a liquid–liquid interface (here wax–water interface) to lowering the total free energy [42]. Thus, SiNPs were firmly adsorbed at the wax–water interface of Pickering emulsion at 75 °C. Meanwhile, the cationic surfactant DDAB was used to make the silica nanoparticles more hydrophobic, causing them to penetrate much deeper into the wax phase [34]. After the emulsion was cooled down, the paraffin wax solidified so that most of the SiNPs were trapped on the surface of wax colloidosomes (Fig. 2). Further, the exposed side of the silica nanoparticle was modified by the in situ hydrolysis of BIBB–APTES synthesized before. The surface of SiNPs was grafted with initiator groups which were used for growing polymer chains. The other side of the SiNPs was well protected by wax to maintain the free hydroxyl groups.

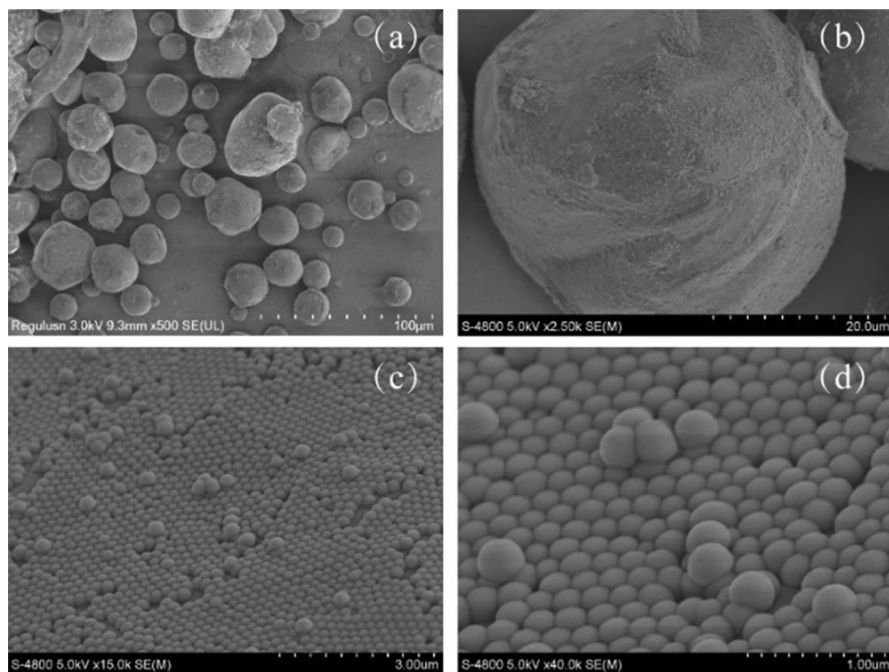
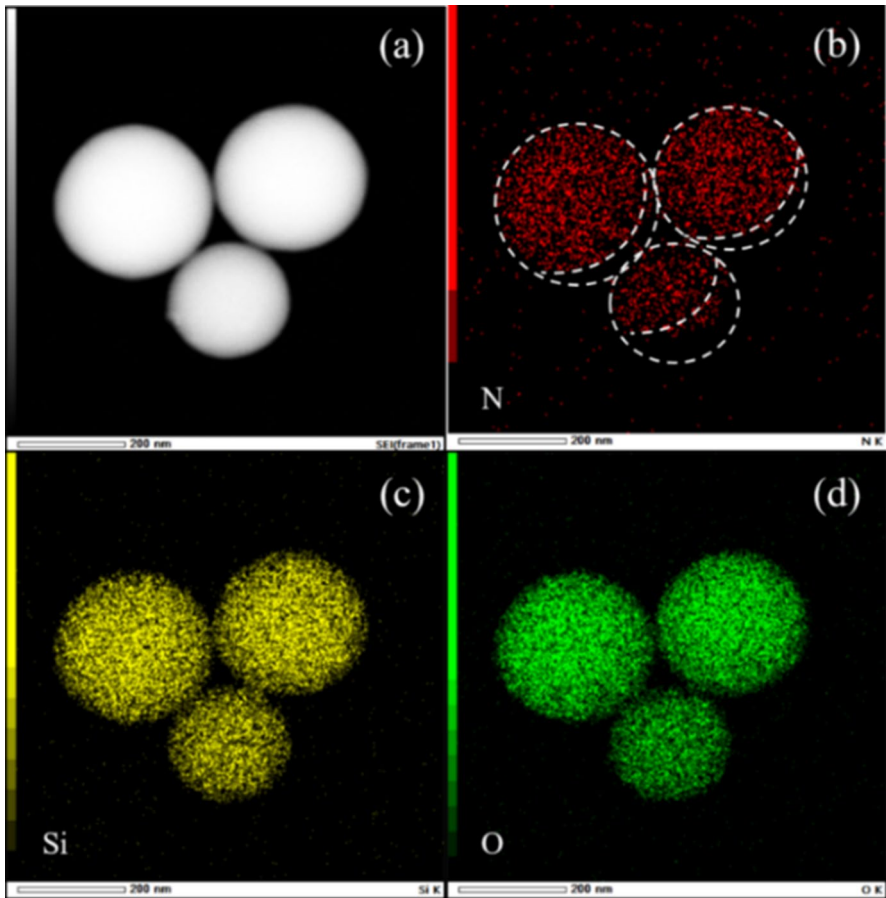


Fig. 2 SEM images of SiNPs located on the surface of paraffin droplets at different magnification






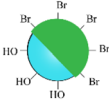
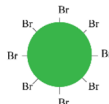
**Fig. 3** TEM image (a) and STEM–EDX mapping images of N (b), Si (c), O (d) elements on the surface of the initiator-modified Janus SiNPs (HO–SiNP–Br)

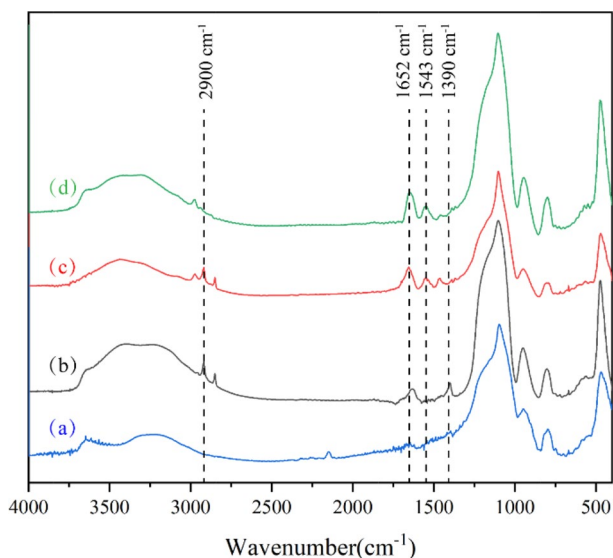
### Characterization of the initiator-modified Janus SiNPs (HO–SiNP–Br)

To further demonstrate the Janus structure of the initiator-modified nanoparticles obtained by the above asymmetrical modification method, SEM–EDX was used to analyze the element distribution of these nanoparticles. As shown in Fig. 3, the distribution of O and Si elements is uniform at the surface of the initiator-modified Janus HO–SiNP–Br particles, but the N element (contained in BIBB–APTES) is distributed asymmetrically. It clearly shows that the silica particles were partially modified by the BIBB–APTES.

For a comparison, symmetric initiator-modified SiNP–Br particles were also synthesized. The Zeta potentials of both the Janus HO–SiNP–Br particles and the symmetric SiNP–Br particles were analyzed. As listed in Table 1, the Zeta potential of bare silica nanoparticles at pH=7 is  $-25.5$  mV. At the same conditions,

**Table 1** The Zeta potential of different silica nanoparticles (bare SiNPs, Janus HO-SiNP-Br particles, symmetric SiNP-Br particles) at pH=7 and their structure illustration

Sample	SiNPs	HO-SiNP-Br	SiNP-Br
Zeta Potential (mV)	-25.5	-33.2	-50.7
Structure			

**Fig. 4** FTIR spectrum of (a) bare SiNPs, (b) Janus HO-SiNP-Br particles, (c) Janus HO-SiNP-PNIPAM particles and (d) symmetric SiNP-PNIPAM particles

the Zeta potential of the symmetric SiNP-Br particles is  $-50.7$  mV, while that of Janus HO-SiNP-Br particles is  $-33.2$  mV. The fewer -Br groups on the surface of HO-SiNP-Br than SiNP-Br should be the reason for its less negative Zeta potential. The results further confirm the asymmetric structure of HO-SiNP-Br.

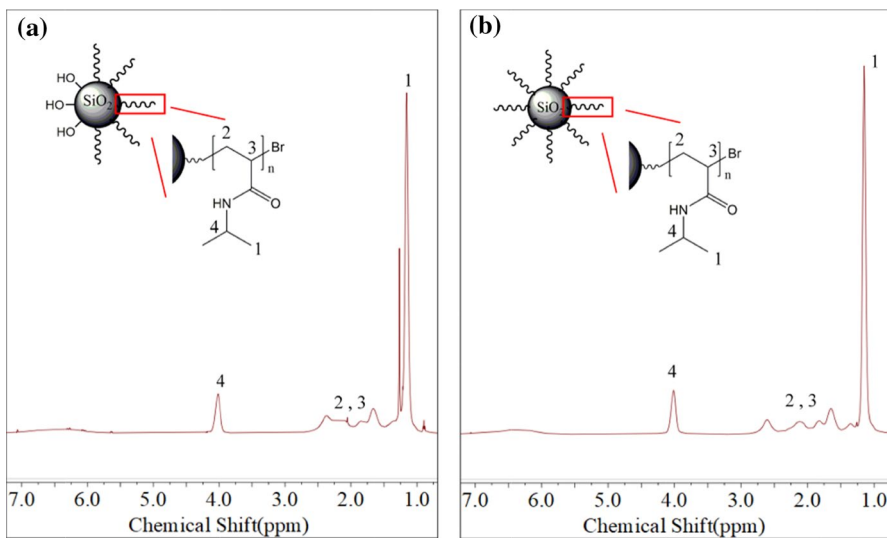
FTIR spectra results are used to verify the structure of silica nanoparticles with BIBB-APTES. Figure 4 shows the FTIR spectrum of the bare SiNPs and Janus HO-SiNP-Br initiator. For bare SiNPs (Fig. 4a), the characteristic absorption peaks of tetrahedron silica structures are observed at  $1078$   $\text{cm}^{-1}$  (Si-O stretching),  $465$   $\text{cm}^{-1}$  (Si-O bending),  $952$   $\text{cm}^{-1}$  (Si-OH bending) and  $800$   $\text{cm}^{-1}$  (Si-O-Si bending). Compared with the bare silica nanoparticles, the asymmetric surface modified with BIBB-APTES introduces additional alkyl groups on the silica surface. Due to the stretching vibration of the C-H group, the Janus HO-SiNP-Br particle (Fig. 4b) has an enhanced band at  $2900$   $\text{cm}^{-1}$ . And the absorption peak at  $1390$   $\text{cm}^{-1}$  is from

the methyl group on 2-bromoisobutyryl chain. All these FTIR results can certify the successful modification of BIBB-APTES on the silica surface.

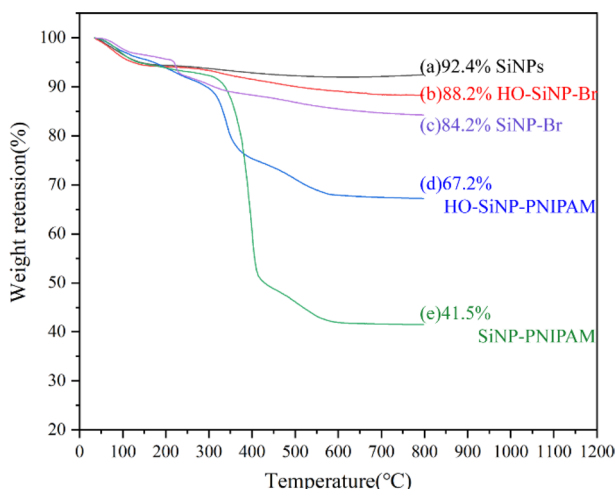
### Characterization of the PNIPAM-modified silica nanoparticles

PNIPAM was grafted on the surface of silica nanoparticles via the SET-LRP process, the mechanism of which was described in Scheme S1. Figure 1b, d describes the TEM and SEM images of PNIPAM-modified Janus SiNPs, respectively. In comparison with the bare SiNPs, the silica nanoparticles modified with PNIPAM are obviously wrapped by polymer layers, which leads to the linkage of the neighbor silica nanoparticles. From the TEM images of the HO-SiNP-PNIPAM particles (Fig. 1d), the Janus structure is demonstrated according to the partial coverage of the brush-like structure on the silica surface. The brush-like material coated on one side of the particles should be the polymer chains of PNIPAM, while the other side is still occupied by free hydroxyl groups, which have no effect on the polymerization of NIPAM.

FTIR spectrum of the Janus HO-SiNP-PNIPAM particles and symmetric SiNP-PNIPAM particles is displayed in Fig. 4c and d. For both the PNIPAM-coated Janus and symmetric nanoparticles, the amide I band ( $1652\text{ cm}^{-1}$ , C=O stretching) and amide II band ( $1543\text{ cm}^{-1}$ , N-H stretching) can be clearly observed, indicating the successful grafting of PNIPAM on silica nanoparticles.  $^1\text{H}$  NMR results (Fig. 5) also confirm the conclusion above. Peak 1 at  $\delta \sim 1.1$  comes from the methyl H in the isopropyl group of the PNIPAM branch. The multiplets ( $\delta 1.7\text{--}2.5$ ) belong to the protons of the units  $(\text{CHCH}_2)_n$  on PNIPAM chains and the characteristic H peaks



**Fig. 5**  $^1\text{H}$  NMR spectrum of (a) Janus HO-SiNP-PNIPAM particles and (b) symmetric SiNP-PNIPAM particles



**Fig. 6** TGA analysis of (a) origin SiNPs, (b) Janus HO-SiNP-Br particles, (c) symmetric SiNP-Br particles, (d) Janus HO-SiNP-PNIPAM particles and (e) symmetric SiNP-PNIPAM particles

of CH can be clearly found at  $\delta \sim 4.0$  (Peak 4). The integration ratio of Peak 1–4 is about 5.8: 1, which represents 6 protons and 1 proton at positions 1 and 4, respectively. All of these results demonstrate the coating of PNIPAM on silica.

TGA analysis was used to further confirm the successful grafting of PNIPAM, which was conducted in air atmosphere at a heating speed of 10 °C/min from 25 to 800 °C. As shown in Fig. 6a, the weight retention of bare SiNPs at 800 °C is ~92.4 wt%. And the weight retention is about 88.2% for Janus HO-SiNP-Br particles (Fig. 6b), which is apparently lower than the bare silica nanoparticles. It can be estimated that the amount of initiator grafted onto the surface of SiNPs is ~4.2 wt%. The weight retention of Janus HO-SiNP-PNIPAM particles is ~67.2 wt% (Fig. 6d). Thus, the polymer mass content relative to the silica core is calculated to be ~21.0 wt%. Using the same method, for symmetric SiNP-PNIPAM particles (Fig. 6c and e), the mass contents of the initiator and polymer can be calculated as ~8.2 wt% and ~42.7 wt%, respectively. These TGA results reveal the successful graft of PNIPAM chains on the surface of SiNPs, and the polymer content of Janus silica nanoparticles is much lower than that of symmetrically modified SiNPs due to the fewer initiating sites on Janus initiators. To obtain the molecular weight and molecular weight distribution of grafted PNIPAM chains, Janus HO-SiNP-PNIPAM and symmetric SiNP-PNIPAM were etched with hydrofluoric acid to cleave the grafted PNIPAM chains for further GPC analysis. TGA and GPC results of PNIPAM chains grafted on different silica nanoparticles are summarized in Table 2. The molecular weight ( $M_w$ ) of grafted PNIPAM on Janus HO-SiNP-PNIPAM and symmetric SiNP-PNIPAM was 2388 g/mol and 2548 g/mol, respectively.

When nanoparticles adsorb at the oil-water interface of Pickering emulsions, the contact angle ( $\theta$ ) is determined by their hydrophilic and hydrophobic balance. Thus, the contact angle at the oil-particle-water interface is usually used to characterize the hydrophilicity of nanoparticles. When  $\theta < 90^\circ$ , the nanoparticles show hydrophilicity and would immerse in the aqueous phase to form an oil-in-water (o/w) emulsion, while

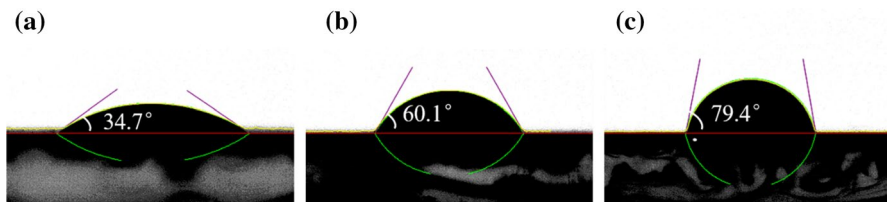
**Table 2** Summary of TGA and GPC results of PNIPAM chains grafted on different silica nanoparticles

Sample	Weight ratio/wt%	Molecular weight of grafted PNIPAM chains ( $M_w$ )/g·mol <sup>-1</sup>	Molecular weight distribution (PDI)
HO-SiNP-PNIPAM	21.0	2388	1.6
SiNP-PNIPAM	41.7	2548	1.8

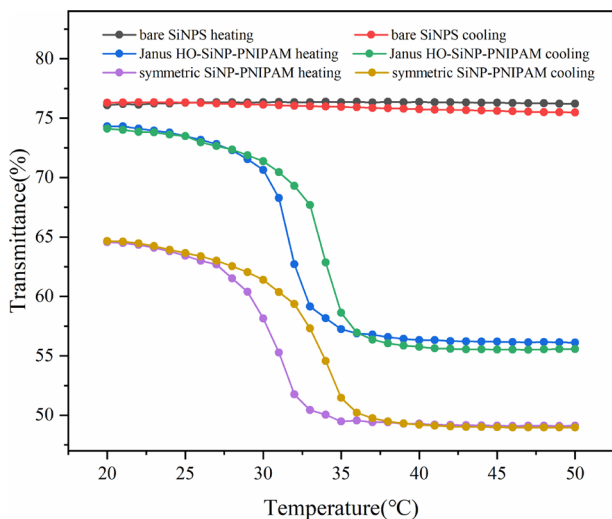
hydrophobic nanoparticles with  $\theta > 90^\circ$  usually form a water-in-oil (w/o) emulsion. To obtain the hydrophilic and hydrophobic of the surfactants, we characterized the contact angle of bare silica nanoparticles, Janus HO-SiNP-PNIPAM nanoparticles and symmetric SiNP-PNIPAM nanoparticles. As shown in Fig. 7, bare silica nanoparticle has the smallest contact angle of  $34.7^\circ$ , and the contact angle of SiNP-PNIPAM is larger than that of HO-SiNP-PNIPAM, indicating that Janus HO-SiNP-PNIPAM nanoparticle is more hydrophilic than symmetric SiNP-PNIPAM nanoparticle.

### Thermo-responsive behavior of PNIPAM-coated Janus and symmetrical nanoparticles

To find out the temperature-responsive behavior of PNIPAM-coated nanoparticles with different spatial structures (symmetrical or asymmetrical modification), their aqueous solutions were tested in UV-Vis spectrophotometer at 500 nm for comparison. Figure 8 indicates the temperature-induced optical transmittance of various nanoparticle aqueous solutions (0.01 wt%). Obviously, the transmittance of bare silica nanoparticles solution has no change with increasing temperature, indicating that bare silica nanoparticles do not have temperature-responsive performance. While the two aqueous solutions of Janus HO-SiNP-PNIPAM and symmetric SiNP-PNIPAM both have a sudden change in optical transmittance with the increasing of temperature, and the solutions became transparent again when they are cooled down. This finding shows that thermo-response behavior is reversible and recycled. At low temperature, the initial optical transmittance of the aqueous solutions is  $\sim 75\%$  and  $\sim 65\%$ , respectively, for Janus HO-SiNP-PNIPAM and symmetric SiNP-PNIPAM nanoparticles. At the same concentration, the Janus HO-SiNP-PNIPAM aqueous solution is a little more transparent than the symmetric SiNP-PNIPAM nanoparticle, which is consistent with the results of contact angle (Fig. 7). It could be caused by the hydrogen bond formed between silanol and water at low temperatures, increasing the hydrophilicity of



**Fig. 7** The contact angle of (a) bare silica nanoparticles; (b) asymmetric HO-SiNP-PNIPAM nanoparticles and (c) symmetric SiNP-PNIPAM nanoparticles

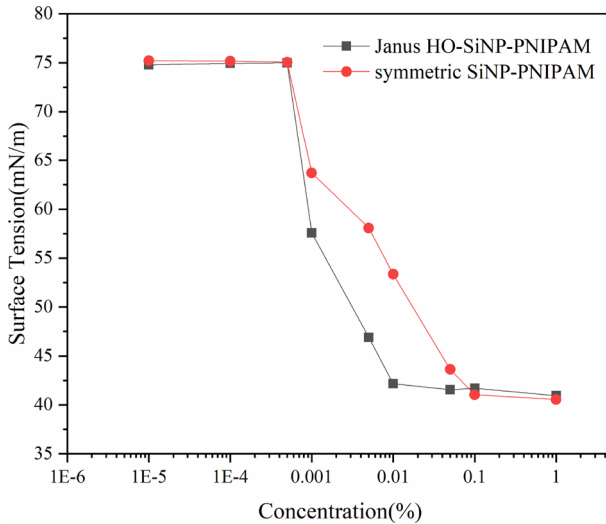


**Fig. 8** The optical transmittance acquired from aqueous solutions (0.01 wt%) of bare SiNPs, Janus HO-SiNP-PNIPAM and symmetric SiNP-PNIPAM particles at 500 nm

the Janus nanoparticles. As a result, the phase transition temperature for the Janus and symmetric nanoparticles is about 32–35 °C and 30–32 °C, respectively. For symmetric SiNP-PNIPAM, the hydrogen bond between –NH– and C=O groups on PNIPAM chains and water are broken and PNIPAM chains go through a coil-globule transition when the temperature reaches upon LCST of PNIPAM, leading to the agglomeration of the nanoparticles [43]. However, for Janus particles, the hydrogen bond between silanol and water is still available with temperature increasing, when the hydrogen bonds between PNIPAM chains and water are destroyed (Figure S1). The presence of silanol on one side of the Janus nanoparticles endows its extra hydrophilicity at a higher temperature. Thus, a higher phase transition temperature is observed.

Figure 9 shows the surface tension of Janus HO-SiNP-PNIPAM and symmetrical SiNP-PNIPAM nanoparticles solution with different concentrations at 25 °C. For Janus nanoparticles solution, the surface tension decreases from 75 to 40 mN/m with the concentration increasing from  $1 \times 10^{-5}$  to 0.01 wt%. After that, the surface tension basically remains unchanged with the increasing concentration. Similarly, with the concentration increasing from  $1 \times 10^{-5}$  to 0.1 wt%, the surface tension of symmetric nanoparticles solution decreases from 75 to 40 mN/m, followed by a stable surface tension result. It indicated that when the concentration is less than  $5 \times 10^{-5}$  wt%, the amount of thermo-responsive nanoparticles in the solution are too small to reduce the surface tension. In this case, there is basically no difference between the surfactant solution and water. After that, when the concentration is increasing, the nanoparticles are enough to be well adsorbed on the surface of the aqueous solution, which can significantly reduce the surface tension of water. When the concentration of Janus nanoparticles solution is increased to 0.01 wt% (0.1 w% for symmetric nanoparticles solution), nanoparticles adsorbed at the interface reach

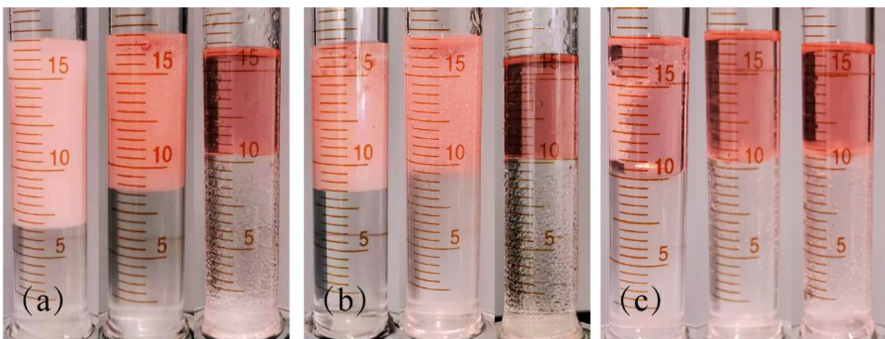




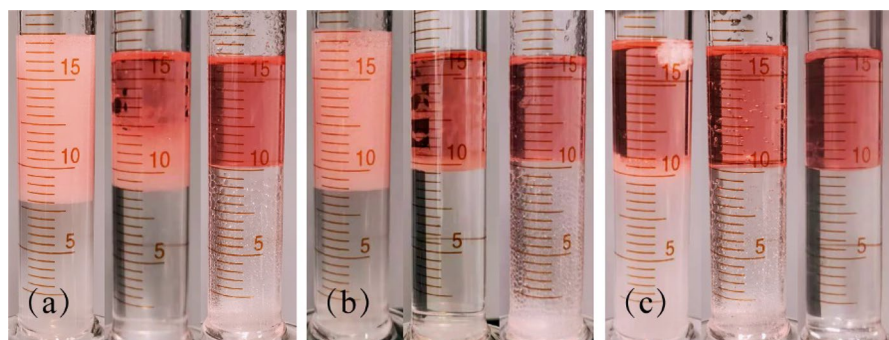
**Fig. 9** Surface tension of Janus HO-SiNP-PNIPAM and symmetric SiNP-PNIPAM particles solution at 25 °C

saturation; thus, the surface tension no longer decreases. It confirms that the Janus nanoparticles are effective as surfactant when concentration is higher than 0.01 wt%. However, symmetric nanoparticles can be used as a thermo-responsive surfactant with a concentration more than 0.1 wt%, which is much higher than that of the Janus HO-SiNP-PNIPAM particles. The surface tension results indicate that the Janus particles are superior to the symmetrical SiNP-PNIPAM nanoparticles in surface activity.

The emulsification experiment of the oil/water system was conducted at both low and high temperatures by using tetradecane ( $C_{14}$ ) as the model oil. Various Janus nanoparticles and symmetric nanoparticles solutions with different concentrations



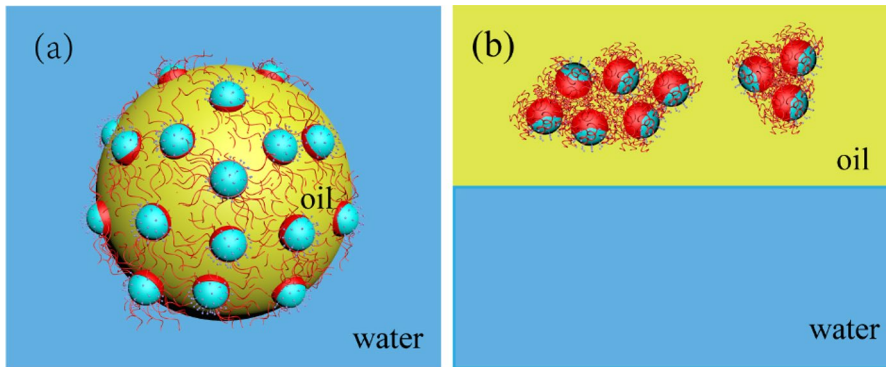
**Fig. 10** The  $C_{14}$ /water system (with 1:2 mass ratio) with 0.1 wt%, 0.01 wt% and 0.001 wt% (from left to right) Janus HO-SiNP-PNIPAM solutions: (a) the emulsification at 25 °C; (b) the emulsification maintained for 12 h; (c) the demulsification at 50 °C maintained for 10 min



**Fig. 11** The  $C_{14}$ /water system (with 1:2 mass ratio) of 0.1 wt%, 0.01 wt% and 0.001 wt% (from left to right) symmetric SiNP–PNIPAM solutions: (a) the emulsification at 25 °C; (b) the emulsification maintained for 12 h; (c) the demulsification at 50 °C maintained for 10 min

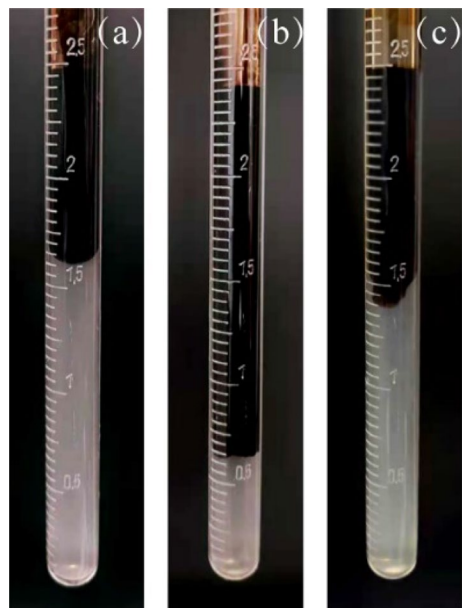
(0.1 wt%, 0.01 wt% and 0.001 wt%) were prepared and used to make the  $C_{14}$ /water system (mass ratio of 1:2). Tetradecane was dyed with Sudan IV to make a distinction between the oil phase and water. The emulsification was conducted at 25 °C and remained stable for 12 h. With the temperature increasing to 50 °C, demulsification occurs after about 10 min. Figures 10 and 11 show the emulsification and demulsification of Janus and symmetric nanoparticles solution with three different concentrations, respectively. It can be observed from Fig. 10 that Janus nanoparticles solutions with a concentration of 0.1 wt% or 0.01 wt% can form a stable emulsion after the homogenization, while those with a concentration of 0.001 wt% cannot. It indicates that 0.001 wt% surfactant particles in a solution are not enough for the formation of a dense and stable surfactant film at the interface, which is consistent with the surface tension results. For symmetric nanoparticle solutions, only 0.1 wt% solutions can form a stable emulsion, while others cannot (Fig. 11). According to surface tension results of SiNP–PNIPAM nanoparticles, the surface tension of the solution is basically the same as water when the concentration is less than 0.1 wt%. It means that the adsorption of the symmetrical nanoparticles on the oil–water interface is rather difficult. As shown in Fig. 10c and Fig. 11c, demulsification occurred upon 50 °C rapidly. The hydrogen bond between the PNIPAM chain and water was broken under high temperature, causing the collapse of PNIPAM chains and the demulsification of the oil/water emulsion (Fig. 12).

To investigate the potential application of the PNIPAM-coated nanoparticles, the thermo-responsive properties were further evaluated in a crude oil/water system. The system was constructed by Saudi crude oil and 0.1 wt% Janus or symmetric nanoparticles solution. As shown in Fig. 13, Saudi crude oil can be emulsified at 25 °C by Janus HO–SiNP–PNIPAM solution, and the emulsion is stabilized for more than 24 h. Similar to the tetradecane/water system, demulsification occurs when the temperature is increased to 50 °C. These results could provide important clues that PNIPAM-coated nanoparticles can be used as a temperature-sensitive surfactant and have the possibility of emulsification and demulsification in crude oil–water systems.



**Fig. 12** The mechanism for the thermo-responsive performance of Janus HO-SiNP-PNIPAM particles: (a) emulsified at 25 °C; (b) demulsified at 50 °C

**Fig. 13** The Saudi crude oil and 0.1 wt% Janus HO-SiNP-PNIPAM solutions: (a) before emulsification at 25 °C, (b) after emulsification at 25 °C and (c) after demulsification at 50 °C



## Conclusion

In this work, the temperature-sensitive polymer PNIPAM was successfully grafted onto silica nanoparticles by the SET-LRP method. Two kinds of PNIPAM-modified silica nanoparticles with different spatial structures (Janus and symmetric) were synthesized. Both the two kinds of nanoparticles have temperature-sensitive performance. However, in comparison with silica nanoparticles uniformly coated by PNIPAM chains, Janus PNIPAM-modified nanoparticles in this study exhibited a higher phase transition temperature, due to the formation of hydrogen bonds between the

hydroxyl groups and water. The emulsification and demulsification experiments of tetradecane–water systems showed that Janus HO–SiNP–PNIPAM had superior emulsification performance and can form an emulsion at a lower concentration (0.01 wt%) than symmetric SiNP–PNIPAM. The application the Janus nanoparticles in the crude oil/water system demonstrate that the PNIPAM-coated nanoparticles have an excellent thermal-responsive properties, of which the emulsion can be formed at room temperature and demulsified at elevated temperatures. In summary, the as-prepared PNIPAM-modified Janus silica nanoparticles show an ideal application perspective in industrial fields.

**Supplementary Information** The online version contains supplementary material available at <https://doi.org/10.1007/s11164-021-04486-8>.

**Acknowledgements** This work is financially supported by the National Natural Science Foundation of China (41672045) as well as the Foundation of PetroChina on Basic Research and Strategic Reserve Technology Research (2017D-5008-03).

## References

1. P.G. de Gennes, *Science* **256**, 495 (1992)
2. T. Yang, L. Wei, L. Jing, J. Liang, X. Zhang, M. Tang, M.J. Monteiro, Y.I. Chen, Y. Wang, S. Gu, D. Zhao, H. Yang, J. Liu, G.Q.M. Lu, *Angew. Chem. Int. Ed. Engl.* **56**, 8459 (2017)
3. W. Qin, T. Peng, Y. Gao, F. Wang, X. Hu, K. Wang, J. Shi, D. Li, J. Ren, C. Fan, *Angew. Chem. Int. Ed. Engl.* **56**, 515 (2017)
4. F. Wang, G.M. Pauletti, J. Wang, J. Zhang, R.C. Ewing, Y. Wang, D. Shi, *Adv. Mater.* **25**, 3485 (2013)
5. D. Yi, Q. Zhang, Y. Liu, J. Song, Y. Tang, F. Caruso, Y. Wang, *Angew. Chem. Int. Ed. Engl.* **55**, 14733 (2016)
6. Y.H. Hwang, K. Jeon, S.A. Ryu, D.P. Kim, H. Lee, *Small.* **16**, 2005159 (2020)
7. H. Wu, K. Gao, Y. Lu, Z. Meng, C. Gou, Z. Li, M. Yang, M. Qu, T. Liu, J. Hou, W. Kang, *Coll. Surf. A: Physicochem. Eng. Aspects* **586**, 124162 (2020)
8. F. Amani, E. Dehghani, M. Salami-Kalajahi, *J. Polym. Res.* **28**, 142 (2021)
9. S. Berger, A. Snytska, L. Ionov, K.J. Eichhorn, M. Stamm, *Macromolecules* **41**, 9669 (2008)
10. L. Qi, C. Song, T. Wang, Q. Li, G.J. Hirasaki, R. Verduzco, *Langmuir* **34**, 6522 (2018)
11. C.F. Ma, X.B. Bi, T. Ngai, G.Z. Zhang, *J. Mater. Chem. A* **1**, 5353 (2013)
12. J. Jiang, Y. Ma, Z. Cui, B.P. Binks, *Langmuir* **32**, 8668 (2016)
13. N. Lai, Q. Zhu, D. Qiao, K. Chen, D. Wang, L. Tang, G. Chen, *Front. Chem.* **8**, 112509 (2020)
14. P. Yao, A. Zou, Z. Tian, W. Meng, X. Fang, T. Wu, J. Cheng, *Coll. Surf. B-Biointerfaces* **198**, 125266 (2021)
15. S. Bjorkegren, M.C.A. Freixiela Dias, K. Lundahl, L. Nordstierna, A. Palmqvist, *Langmuir* **36**, 2357 (2020)
16. Z.P. Du, X.F. Sun, X.M. Tai, G.Y. Wang, X.Y. Liu, *Appl. Surf. Sci.* **329**, 234 (2015)
17. A. Alkan, S. Wald, B. Louage, B.G. De Geest, K. Landfester, F.R. Wurm, *Langmuir* **33**, 272 (2017)
18. Y. Takahashi, N. Koizumi, Y. Kondo, *Langmuir* **32**, 7556 (2016)
19. J.F. Lutz, O. Akdemir, A. Hoth, *J. Am. Chem. Soc.* **128**, 13046 (2006)
20. H.G. Schild, *Prog. Polym. Sci.* **17**, 163 (1992)
21. O. Holderer, S. Maccarrone, S. Pasini, M.S. Appavou, A. Gelissen, *Result. Phys.* **21**, 103805 (2021)
22. F. Chen, C. Dong, C. Chen, W.D. Yin, W. Zhai, X.Y. Ma, B. Wei, *Ultrason. Sonochem.* **58**, 104705 (2019)
23. T. Wu, Y.F. Zhang, X.F. Wang, S.Y. Liu, *Chem. Mater.* **20**, 101 (2008)
24. B.P. Binks, P.D.I. Fletcher, *Langmuir* **17**, 4708 (2001)
25. B. Dong, B. Li, C.Y. Li, *J. Mater. Chem.* **21**, 13155 (2011)

26. B. Wang, B. Li, R.C. Ferrier Jr., C.Y. Li, *Macromol. Rapid. Commun.* **31**, 169 (2010)
27. T. Zhou, B. Wang, B. Dong, C.Y. Li, *Macromolecules* **45**, 8780 (2012)
28. B. Haney, J.G. Werner, D.A. Weitz, S. Ramakrishnan, *Soft Matter* **16**, 3613 (2020)
29. C. Tang, C.L. Zhang, J.G. Liu, X.Z. Qu, J.L. Li, Z.Z. Yang, *Macromolecules* **43**, 5114 (2010)
30. L. Qu, H. Hu, J. Yu, X. Yu, J. Liu, Y. Xu, Q. Zhang, *Langmuir* **33**, 5269 (2017)
31. X. Wang, X. Feng, G. Ma, L. Yao, M. Ge, *Adv. Mater.* **28**, 3131 (2016)
32. D. Gao, M. Zhang, B. Lyu, J. Ma, Y. Li, *Coll. Surf. A: Physicochem. Eng. Aspects* **607**, 125295 (2020)
33. L. Hong, S. Jiang, S. Granick, *Langmuir* **22**, 9495 (2006)
34. S. Jiang, S. Granick, *Langmuir* **24**, 2438 (2008)
35. S. Jiang, M.J. Schultz, Q. Chen, J.S. Moore, S. Granick, *Langmuir* **24**, 10073 (2008)
36. Z. Chu, B. Zhong, W. Zhou, P. Cui, J. Gu, B. Tian, O.S. Olasoju, X. Zhang, W. Sun, *Coll. Surf. A: Physicochem. Eng. Aspects* **603**, 125183 (2020)
37. E. Sharifzadeh, M. Salami-Kalajahi, M.S. Hosseini, M.K.R. Aghjeh, *Coll. Polym. Sci.* **295**, 25 (2016)
38. X. Wang, M. Zeng, Y.H. Yu, H. Wang, M.S. Mannan, Z. Cheng, *ACS Appl Mater Interfaces* **9**, 7852 (2017)
39. D. Mendez-Gonzalez, P. Alonso-Cristobal, E. Lopez-Cabarcos, J. Rubio-Retama, *Eur. Polym. J.* **75**, 363 (2016)
40. W. Stöber, A. Fink, E. Bohn, *J. Colloid Interface Sci.* **26**, 62 (1968)
41. X.D. Wang, Z.X. Shen, T. Sang, X.B. Cheng, M.F. Li, L.Y. Chen, Z.S. Wang, *J. Coll Interface. Sci.* **341**, 23 (2010)
42. R. Aveyard, B.P. Binks, J.H. Clint, *Adv. Coll. Interface Sci.* **100**, 503 (2003)
43. T. Serizawa, K. Wakita, M. Akashi, *Macromolecules* **35**, 10 (2002)

**Publisher's Note** Springer Nature remains neutral with regard to jurisdictional claims in published maps and institutional affiliations.